Neurobiology of Disease

Inhibition of Amyloid-β (Aβ) Peptide-Binding Alcohol Dehydrogenase-Aβ Interaction Reduces Aβ Accumulation and Improves Mitochondrial Function in a Mouse Model of Alzheimer's Disease

Jun Yao,[1] **Heng Du,**[1] **Shiqiang Yan,**[1] **Fang Fang,**[1] **Chaodong Wang,**[1] **Lih-Fen Lue,**[2] **Lan Guo,**[1] **Doris Chen,**[1] **David M. Stern,**[3] **Frank J. Gunn Moore,**[4] **John Xi Chen,**[5] **Ottavio Arancio,**[1] **and Shirley ShiDu Yan**[1]

[1]Departments of Pathology and Surgery, Taub Institute for Research on Alzheimer Disease and the Aging Brain, Columbia University, New York, New York 10032, [2]Sun Health Research Institute, Sun City, Arizona 85351, [3]College of Medicine, University of Cincinnati, Cincinnati, Ohio 45229, [4]School of Biology, University of St Andrews, St Andrews KY16 9TF, United Kingdom, and [5]Department of Neurology, Memorial Sloan-Kettering Cancer Center, New York, New York 10065

Amyloid-β (Aβ) peptide-binding alcohol dehydrogenase (ABAD), an enzyme present in neuronal mitochondria, exacerbates Aβ-induced cell stress. The interaction of ABAD with Aβ exacerbates Aβ-induced mitochondrial and neuronal dysfunction. Here, we show that inhibition of the ABAD-Aβ interaction, using a decoy peptide (DP) *in vitro* and *in vivo*, protects against aberrant mitochondrial and neuronal function and improves spatial learning/memory. Intraperitoneal administration of ABAD-DP [fused to the transduction of human immunodeficiency virus 1-transactivator (Tat) protein and linked to the mitochondrial targeting sequence (Mito) (TAT-mito-DP) to transgenic APP mice (Tg mAPP)] blocked formation of ABAD-Aβ complex in mitochondria, increased oxygen consumption and enzyme activity associated with the mitochondrial respiratory chain, attenuated mitochondrial oxidative stress, and improved spatial memory. Similar protective effects were observed in Tg mAPP mice overexpressing neuronal ABAD decoy peptide (Tg mAPP/mito-ABAD). Notably, inhibition of the ABAD-Aβ interaction significantly reduced mitochondrial Aβ accumulation. In parallel, the activity of mitochondrial Aβ-degrading enzyme PreP (presequence peptidase) was enhanced in Tg mAPP mitochondria expressing the ABAD decoy peptide. These data indicate that segregating ABAD from Aβ protects mitochondria/neurons from Aβ toxicity; thus, ABAD-Aβ interaction is an important mechanism underlying Aβ-mediated mitochondrial and neuronal perturbation. Inhibitors of ABAD-Aβ interaction may hold promise as targets for the prevention and treatment of Alzheimer's disease.

Introduction

Amyloid-β peptide (Aβ) has been assigned a central role in the pathogenesis of Alzheimer's disease (AD). Mitochondrial dysfunction occurs in early AD. Aberrant mitochondrial function is known to contribute to alterations in energy metabolism, free radical generation, and cellular calcium homeostasis, all of which are relevant to the pathogenesis of AD (Davis et al., 1997; Sheehan et al., 1997; Humphries and Szweda, 1998; Blass, 2000; Maurer et al., 2000; Hirai et al., 2001; Bosetti et al., 2002; Floyd and Hensley, 2002; Beal, 2004; Yan and Stern, 2005; Devi et al., 2006; Lin and Beal, 2006; Shukkur et al., 2006; Yao et al., 2009). Recent studies have highlighted the significance of the accumulation of Aβ within mitochondria (Lustbader et al., 2004; Caspersen et al.,

2005; Lin and Beal, 2006; Manczak et al., 2006; Yan et al., 2006; Du et al., 2008; Hansson Petersen et al., 2008; Yao et al., 2009). Aβ progressively accumulates in brain mitochondria of Alzheimer's patients and transgenic mouse model of AD, exerting a deleterious effect on mitochondrial function, including energy failure, altered mitochondrial properties, and elaboration of reactive oxygen species (ROS). However, the key intracellular mechanisms through which Aβ impairs cellular properties, resulting in neuronal dysfunction and mitochondrial damage, have yet to be clearly identified.

ABAD (Aβ-binding alcohol dehydrogenase) is a mitochondrial enzyme whose unique features include a broad repertoire of substrates, binding Aβ in the nanomolar range, and potentiating Aβ-induced cell stress. ABAD is elevated in the cerebral cortex and hippocampus of AD-affected brain regions and in mouse models of AD (Yan et al., 1997; He et al., 2002; Lustbader et al., 2004; Chen and Yan, 2007; Yao et al., 2009). Further, the ABAD-Aβ complex was found in brain mitochondria of transgenic (Tg) mice with neuron-targeted overexpression of mutant human amyloid precursor protein (Tg mAPP) and Tg mAPP mice that overexpress ABAD (Tg mAPP/ABAD) (Lustbader et

al., 2004; Takuma et al., 2005). Overexpression of ABAD exacerbates Aβ-mediated mitochondrial and neuronal dysfunction, as evidenced by reduced enzyme activity associated with complex IV in the respiratory chain, diminished oxygen consumption, decreased brain glucose utilization, decreased ATP, and leakage of mitochondrial-derived ROS. Subsequently, double Tg mAPP/ABAD mice exhibit an earlier onset of impaired spatial learning/memory and regional neuropathological changes compared with single Tg mAPP mice. Previously, we have shown that the inhibition of the interaction of Aβ with ABAD (using the ABAD decoy peptide) can suppress expression of both peroxiredoxin II and endophilin I, both of which are elevated in the cerebral cortex of Tg mAPP, Tg mAPP/ABAD mice and human AD patients (Yao et al., 2007; Ren et al., 2008). These data led us to hypothesize that inhibition of the ABAD-Aβ interaction would protect mitochondria and neurons from Aβ-mediated toxicity.

The studies presented herein specifically demonstrate that the introduction of an ABAD-decoy peptide (ABAD-DP) into Tg mAPP mice reduces ABAD-Aβ interaction and protects against Aβ-mediated mitochondrial toxicity. These data provide support for the premise that ABAD-Aβ interaction is a key factor in potentiating Aβ-induced cytotoxicity, and may also be an effective target for therapeutic intervention in AD.

Materials and Methods

Mice. Animal studies were approved by the Animal Care and Use Committee of Columbia University in accordance with the National Institutes of Health guidelines for animal care. Tg mice overexpress a human form of mutant APP that encodes hAPP695-, hAPP751-, and hAPP770-bearing mutations linked to familial AD (V717F, K670M, N671L, J-20 lines) (Mucke et al., 2000). Male mice were used for all the experiments.

Tat-Mito-ABAD-93-116/116-93 peptides synthesis and administration. Tat-Mito-ABAD-93-116 and Tat-Mito-ABAD-116-93 peptides were synthesized by the W. M. Keck Facility, Yale University (New Haven, CT). The sequences of the peptides contain both Tat and Mito (the amino acids of the mitochondrial targeting) in one-letter code as follows: YGRKKRRQRRR for cell-membrane transduction domain of the human immunodeficiency virus 1 (HIV) transactivator protein (Tat); GIAVASKTYNLKKGQTHTLEDFQR for the specific sequence of the human ABAD that encompasses the Aβ binding region (residues 93–116 of ABAD). The mouse mitochondrial targeting sequence, MAAAVRSVKGL, was incorporated between Tat and ABAD-93-116 (DP) and -116-93 [reverse peptide (RP)]. Tat-Mito-ABAD-116-93 was constructed with a reversed amino acid sequence of ABAD (residues 116–93) as the corresponding sequence of ABAD residues 93–116. Mito-ABAD-DP and -RP were labeled with Texas Red (Southern Biotechnology Associates) and added to cultured neurons at a concentration of 10 μM for 30 min. For examination of mitochondrial localization of Texas Red-labeled mito-ABAD peptide, neurons were fixed with 4% paraformaldehyde, incubated with HSP60 antibody for 30 min, followed by FITC-conjugated secondary antibody. To examine entry of ABAD peptide into brain, Texas Red-labeled Tat-Mito-ABAD-DP and -RP were intraperitoneally injected into mice (2.6 mg/kg). At 30 and 120 min after administration of ABAD peptide, mice were perfused with 4% paraformaldehyde and one half of the brains was homogenized immediately and fluorescently quantified Texas Red at excitation of 550 nm and emission of 615 nm wavelengths. The other hemisphere was subjected to immunostaining with Hsp60 antibody to examine localization of Texas Red-labeled ABAD peptide in mitochondria. For the peptide infusion, mice at the age of 7 months were intraperitoneally injected with Tat-mito-ABAD-DP, -RP or vehicle daily for 3 months, and then subjected to experiments.

Generation and characterization of Tg PD-mito-ABAD(92-120) mice. The human ABAD cDNA containing amino acids 92–120 was subcloned into the pECFP-Mito vector (Clontech, CA) using BamHI plus AgeI cloning sites. The transgenic cassettes contain mitochondrial targeting sequence derived from the precursor of subunit VIII of human cytochrome *c* oxidase-ABAD(92-120) and green fluorescence protein (GFP, 27 kDa), which is driven by the platelet-derived growth factor β (PDGF-β) chain promoter. Transgenic expression gene cassettes were generated, isolated as a PvuI fragment, and injected into mouse B6CBAF₁/J oocytes. The oocytes were then implanted into pseudopregnant females, which were subsequently mated with B6CBAF₁/J males, resulting in the generation of three independent founder lines. These founders were backcrossed into the C57BL/6 background strain for eight generations. Transgenic mice were genotyped using the following primers for PCR amplification: 5′-GGATCCGCAGGCATCGCGGT-3′ and 5′-ACCGGTCACATCAAGAACT-3′ for ABAD(92-120), ~92 bp; and 5′-GCTGGTTTAGTGAACCGTCAG-3′ and 5′-TTGTGGCCGTTTAC-GTCGCCGT-3′ for mitochondrial targeting sequence, ABAD(92-120), and N-terminal of GFP, ~353 bp, respectively. Transgene expression was verified by immunoblotting and immunostaining with anti-ABAD antibody. ABAD(92-120) mice were crossed with mAPP mice to generate double Tg mAPP/ABAD(92-120) mice along with littermate single Tg mice [mAPP, ABAD(92-120)], and nontransgenic control mice (non-Tg). Transgenic mice indicated above were aged to 10–11 months old for experiments.

Isolation of brain mitochondria and assays for mitochondrial complex III and IV activities. Mitochondrial fractions were prepared for determination of oxygen consumption using a Clark oxygen electrode as previously described (Caspersen et al., 2005; Du et al., 2008, 2009). Mitochondrial enzyme activity associated with complexes III and IV were measured using biochemical methods as previously described (Birch-Machin and Turnbull, 2001).

Coimmunoprecipitation for detecting mitochondrial Aβ-ABAD complex. Purified mitochondria (500 μg) were incubated with lysis buffer for 15 min on ice and then spun for 10 min at 10,000 × g. Resulting supernatants were immunoprecipitated with mouse anti-Aβ IgG (6E10; 8 μg/ml) (Signet Laboratories) at 4°C overnight, then incubated with protein A/G beads followed by Western blotting with ABAD antibody (1:10,000). Since the expression levels of cytochrome *c* oxidase subunit IV (COX IV) were not significantly changed in Tg mAPP mice compared with that in non-Tg littermates (data not shown), we used COX IV as mitochondrial protein loading controls. Equal amounts of mitochondrial protein used for immunoprecipitation were immunoblotted by mouse anti-COX IV antibody (1:1000; Invitrogen, Eugene, OR).

Immunoblotting, immunostaining, and measurement of AChE activity. Cerebral cortical homogenates from Tg mice were subjected to immunoblotting using monoclonal anti-ABAD (1:8000), 6E10 (1:1000; Signet), or mouse anti-COX IV IgG (1:4000; Sigma). Binding sites of primary antibody were visualized with affinity-purified peroxidase-conjugated goat anti-rabbit IgG or goat anti-mouse IgG (1:5000; Sigma) followed by the addition of ECL substrate (GE Healthcare), and completed with chemiluminescence. Relative intensity of gel bands was quantified using NIH ImageJ software. Immunohistochemistry was performed on mice brain sections. After 6 min of perfusion with saline, brains were fixed in paraformaldehyde (4%) for 26 h. Serial vibratome sectioning (20 μm) was completed and immunocytochemical analyses were performed using rabbit anti-ABAD IgG (10 μg/ml). For on-slide immunohistochemistry, sites of primary antibody binding were visualized using peroxidase-conjugated goat anti-rabbit IgG and 3-amino-9-ethyl carbazole (Sigma) as the detection system. AChE activity was determined histochemically using a commercial kit (Invitrogen). The quantification of images was performed using computer software (Universal Image) to determine the percentage area occupied. To ensure objective assessments and reliability of results, brain sections from mice in any given experiment were blindly coded and processed in parallel. Codes were revealed after the analysis was complete.

Assessment of ROS in vivo. The production of superoxide was measured by monitoring hydroethidine (HEt) (Invitrogen) levels in neurons of mouse brains, as previously described by Murakami et al. (1998). Briefly, 5 mM HEt stock solution was diluted to 1 mg/ml in PBS. Tg mice were intravenously injected with diluted HEt solution (6.7 μg/kg). Thirty minutes later, animals were perfused with 4% paraformaldehyde, immediately followed by cryostat brain sectioning and analysis using confocal

microscopy. Brain sections were processed for immunostaining with anti-Hsp60 (mitochondrial marker) to determine signal localization in mitochondria. Half of these mouse brain tissues were homogenized by 10 strokes in a glass Teflon homogenizer in 1 ml of the brain homogenizing buffer; this was immediately followed by fluorescent quantification in a 96-well microplate with an excitation of 415 nm and emission of 510 nm using a fluorescent microplate reader (Molecular Devices).

4-Hydroxy-2-nonenal (HNE-4) was measured by immunochemistry assay. Brain sections were stained with mouse anti-HNE-4 antibody and the percentage of area occupied by HNE-4 staining in hippocampus was quantified using Universal Image Computer Software.

Behavioral evaluation. Behavioral studies were performed to assess spatial learning and memory in the radial arm water maze as previously described (Arancio et al., 2004; Lustbader et al., 2004; Du et al., 2008). Investigators were blinded to mouse genotypes until completion of behavioral testing. Mice were allowed 60 s to find the hidden platform and errors were counted. Mice that failed to find the platform within 60 s were guided to the hidden platform and stayed on the platform for 10 s. Retention memory was assessed 30 min after the initial water maze experiment.

Aβ degradation assay for determination of PreP activity. Purified mitochondrial matrix PreP (presequence peptidase) protein from Tg mice was incubated with biotin-Aβ1–42 in a degradation buffer containing 20 mM HEPES-KOH, pH 8.0, and 10 mM $MgCl_2$ at 37°C for 3 h. The mixtures were then centrifuged at 4°C and $10,000 \times g$ for 10 min, incubated with avidin agarose to pull down Aβ, and then subjected to immunoblotting. Biotinylation of Aβ1–42 was revealed by extra-avidin-conjugated antibody and ECL. Immunoinactivation was performed by preincubating mitochondrial fractions with 6 μg of antibodies raised against hPreP (provided by Dr. Elzbieta Glasser, Stockholm University, Stockholm, Sweden) at 4°C for 30 min before the addition of biotin-labeled Aβ1-42.

Statistical analyses were performed using StatView software. ANOVA was used for repeated measures followed by Fisher's protected least significant difference for *post hoc* comparisons. Results are expressed as mean ± SEM.

Results

Administration of mito-ABAD-DP prevents ABAD-Aβ complex formation and preserves mitochondrial function in Tg mAPP mice

In view of the potentially key role of ABAD binding to Aβ in Aβ-induced mitochondrial dysfunction, we sought to determine the effect of antagonizing ABAD/Aβ interaction on mitochondrial and neuronal function in an Aβ-rich environment, as provided by a transgenic AD-type mouse model. Amino residues 94–116 of ABAD are considered as major binding sites in ABAD mediating binding to Aβ (Lustbader et al., 2004; Takuma et al., 2005). Thus, we made an ABAD decoy peptide, which we had successfully used previously to block interaction of ABAD with Aβ (Lustbader et al., 2004). The decoy peptide alone is not toxic to the cells (Lustbader et al., 2004). Specifically, to introduce the ABAD peptide inside cells, we used an 11 aa transduction domain of HIV Tat fused with an ABAD(93-116) peptide (ABAD-DP) or its reverse version (ABAD-RP) to allow rapid transduction into intact tissue. To concentrate ABAD-DP within mitochondria, the site of ABAD-Aβ complex formation, a mitochondrial targeting sequence derived from mouse ABAD was also added to Tat-ABAD-DP and -RP. Supplemental Figure S1, *A–G* (available at www.jneurosci.org as supplemental material), shows the mitochondrial localization of ABAD peptide in brain and cultured neurons.

First, we performed immunoprecipitation followed by immunoblotting to demonstrate an ABAD-Aβ complex. Immunoprecipitation of cortical mitochondria with anti-Aβ IgG (6E10), followed by immunoblotting with anti-ABAD IgG that recognizes intact ABAD and the decoy peptide, revealed a strong im-
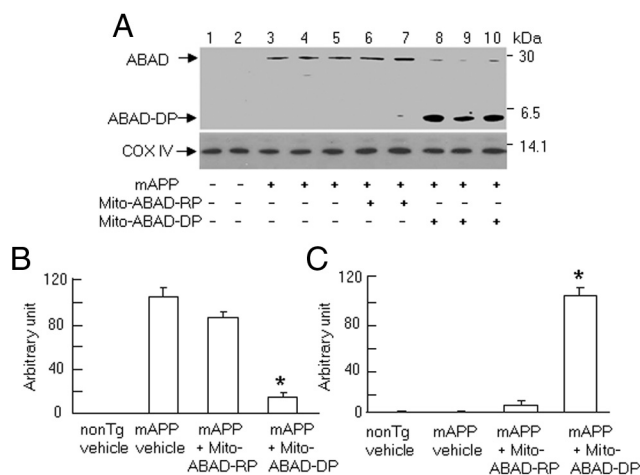
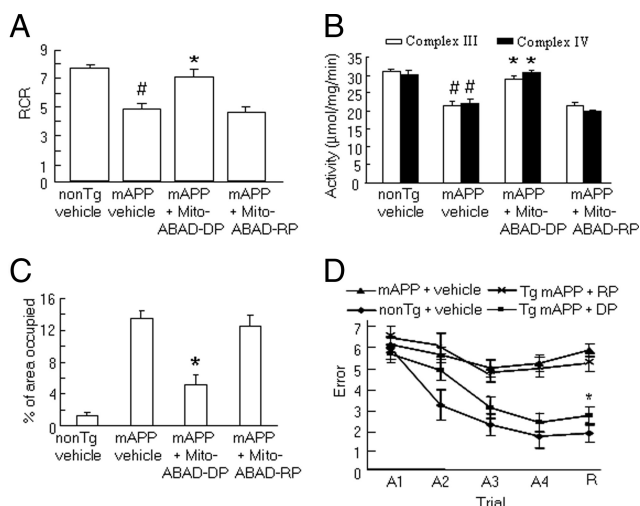**Figure 1.** Effect of systemic administration of mito-ABAD peptide on the formation of ABAD-Aβ complex in Tg mAPP mice. *A*, Brain mitochondria isolated from vehicle-treated non-Tg or Tg mAPP mice, and Tg mAPP mice treated with mito-ABAD-DP or mito-ABAD-RP were subjected to immunoprecipitation with 6E10 antibody followed by immunoblotting with anti-ABAD IgG. Top, Two immunoreactive bands (M_r ~27 and ~5 kDa) were detected. Bottom, Immunoblotting for COX IV showing an equal amount of mitochondrial protein used for the experiments. *B*, *C*, Quantification of intensity of the immunoreactive bands corresponding to M_r ~27 (*B*) and ~5 kDa (*C*). $n = 3$–6 mice per group. *$p < 0.01$ compared with vehicle- or mito-ABAD-RP-treated mAPP mice.

munoreactive band corresponding to M_r ~27 kDa of the endogenous ABAD protein (the latter ABAD was immunoprecipitated in complex with Aβ by the anti-Aβ antibody), in vehicle- and mito-ABAD-RP-treated Tg mAPP mice (Fig. 1*A*, lanes 3–5 and 6–7, respectively), In contrast, two immunoreactive bands (M_r ~27 and ~5 kDa) were detected in cortical mitochondria from mito-ABAD-DP-treated Tg mAPP mice (Fig. 1*A*, lanes 8–10; the 5 kDa band corresponds to immunoreactive ABAD-DP immunoprecipitated in complex with Aβ). The intensity of the immunoreactive band corresponding to M_r ~27 kDa was significantly decreased (due to decreased amounts of intact ABAD in complex with Aβ), whereas a strong immunoreactive band, M_r ~5 kDa (corresponding to increased amounts of Aβ complexed with the ABAD-DP), was observed in cortical mitochondria from Tg mAPP mice treated with mito-ABAD-DP for 3 months (from 7 to 10 months of age) (Fig. 1*A*, lanes 8–10). In contrast, the 5 kDa immunoreactive band was undetectable in mitochondrial extracts from vehicle-treated or mito-ABAD-RP-treated Tg mAPP mice. Mito-ABAD-RP treatment did not disrupt the formation of the ABAD (full-length)-Aβ complex (Fig. 1*A*, lanes 6–7, *B*). Densitometry of combined immunoreactive bands for ABAD/AB and ABAD-DP/Aβ (5 kDa) is shown in Figure 1, *B* and *C*, respectively. These results indicate that mito-ABAD-DP competitively binds mitochondrial Aβ, diminishing ABAD/Aβ complex formation in mitochondria from Tg mAPP mice.

Next, we examined whether inhibition of the ABAD-Aβ interaction by administration of mito-ABAD-DP preserved mitochondrial function. Mitochondrial function was evaluated by measuring the respiratory chain rate, activity of mitochondrial enzymes associated with the respiratory chain, and generation of reactive oxygen species. As shown in Figure 2, *A* and *B*, mitochondria from vehicle-treated Tg mAPP mice exhibited significantly reduced oxygen consumption, and reduced activity of mitochondrial enzymes associated with complexes III and IV. We did not find significant alterations in the expression levels of COX IV in Tg mAPP mice compared with non-Tg mice based on im-

Figure 2. Effect of systemic administration of mito-ABAD peptide on mitochondrial function and spatial memory. ***A***, ***B***, Effect on mitochondrial function. The respiratory control rate (RCR) (***A***), and enzyme activities associated with complexes III and IV (***B***) were determined in the brain mitochondria isolated from the indicated Tg mice. ***C***, Quantification of the area occupied by HNE-4 staining in hippocampus of the indicated Tg mice. $n = 3–8$ mice per group. ***D***, Spatial learning and memory were tested using a radial arm water maze in Tg mAPP mice treated with vehicle, mito-ABAD-DP (DP), or mito-ABAD-RP (RP), and non-Tg mice or Tg mAPP mice treated with vehicle ($n = 7–11$ mice per group). A1–A4 denote the acquisition trials, and R denotes the retention trial. $*p < 0.01$ compared with vehicle- or mito-ABAD-RP-treated Tg mAPP mice. $^\#p < 0.05$ compared with vehicle-treated non-Tg mice.

munoblotting for COX IV (data not shown), which differ from the observation in 3xTg APP mice (Yao et al., 2009). The discrepancy of changes in COX IV expression between Tg mAPP mice and other AD mice (Yao et al., 2009, 2010) could be due to the mouse model, gender, and COX IV antibody to specific subunit used in experiments. Tg mAPP mice treated with mito-ABAD-DP for 3 months starting at 7 months of age, in turn, exhibited preservation of oxygen consumption and complex III/IV activity compared with Tg mAPP treated with vehicle or mito-ABAD-RP (Fig. 2A,B).

Because mitochondria are the major source of ROS generation and it is known that overexpression of ABAD in Tg mAPP mice enhances ROS generation (Lustbader et al., 2004), it was logical to assess the effect of blocking ABAD-Aβ interaction on oxidative stress. As shown in Figure 2C, levels of HNE-4, a marker of oxidized products including lipid and protein, were significantly increased in the hippocampus of vehicle- or mito-ABAD-RP-treated Tg mAPP mice, compared with the vehicle-treated non-Tg littermates. In contrast, mito-ABAD-DP-treated Tg mAPP mice showed greatly reduced levels of HNE-4 (~70%) compared with vehicle-treated Tg mAPP mice. These data indicate that administration of mito-ABAD-DP inhibits interaction of ABAD with Aβ within mitochondria and consequently protects mitochondria from Aβ toxicity.

Administration of Mito-ABAD-DP improves spatial learning/memory in Tg mAPP mice

Next, we evaluated whether the protective effect of mito-ABAD-DP on compromised mitochondrial function in mAPP mice might impact behavioral outcomes. Tg mAPP mice (7 months of age) were treated daily with mito-ABAD-DP for 3 months and then evaluated for radial arm water-maze performance. As expected, vehicle-treated Tg mAPP mice displayed a poorer performance than non-Tg littermates after the second

training trial in the acquisition series (A1–A4) and in the fifth retention trial (R, vehicle-treated Tg mAPP mice: 5–6.5 errors; vehicle-treated-non-Tg: 1–2.5 errors) (Fig. 2D). Administration of mito-ABAD-DP largely reduced the gap between vehicle-treated non-Tg mice (mito-ABAD-DP-treated Tg mAPP: ~2.5 errors) during the acquisition and retention trials. The control peptide (mito-ABAD-RP) did not rescue memory impairment. These studies demonstrate that blockade of ABAD-Aβ interaction improved learning and memory in Tg mAPP mice.

Effect of transgene ABAD(92-120) on ABAD/Aβ interaction and mitochondrial function in Tg mAPP/mito-ABAD mice

The results generated from systemic administration of ABAD peptide (DP) indicate the protective effects of ABAD-DP on mitochondrial and neuronal function in Tg mAPP mice. To further confirm the effects of blocking the ABAD-Aβ interaction and to dissect the role of neuronal ABAD in Aβ-mediated mitochondrial perturbation, we generated transgenic mice with neuronal and mitochondria-targeted expression of ABAD(92-120) that encompasses the binding region of ABAD to Aβ under control of the PDGF-β chain promoter, termed Tg mito-ABAD (supplemental Fig. S2, available at www.jneurosci.org as supplemental material). To assess the effect of transgene [ABAD(92-120)] in an Aβ-rich environment, Tg mito-ABAD mice were crossed with animals expressing a mutant form of human APP driven by PDGF-β chain promoter (Tg mAPP), which are known to have high levels of Aβ in the cerebral cortex and mitochondria (Arancio et al., 2004; Lustbader et al., 2004; Caspersen et al., 2005; Du et al., 2008), mitochondrial and neuronal dysfunction, and impairments in learning/memory (Arancio et al., 2004; Lustbader et al., 2004; Takuma et al., 2005). Double transgenic mice (Tg mAPP/mito-ABAD) display Aβ and ABAD(92-120) in mitochondria, which allowed us to test whether the inhibition complex formation between full-length ABAD and Aβ in mitochondria would occur in the presence of ABAD(92-120) in Tg mAPP/mito-ABAD mice. First, we performed immunoprecipitation of brain mitochondria with anti-Aβ (6E10) followed by immunoblotting with anti-ABAD IgG. The results showed strong immunoreactive bands corresponding to M_r ~27 kDa, a complex of full-length ABAD with Aβ, in Tg mAPP mice (Fig. 3A, lanes 1–3), and M_r ~5 kDa, a complex of ABAD(92-120) with Aβ, in the double Tg mAPP/ABAD(92-120) mice (Fig. 3A, lanes 4–6). Complex formation between full-length ABAD and Aβ, demonstrated as a M_r ~27 kDa ABAD-immunoreactive band was significantly reduced in brain mitochondria of Tg mAPP/mito-ABAD mice compared with the single Tg mAPP mice (Fig. 3A,B). These data indicate that ABAD(92-120) interacts with mitochondrial Aβ, which in turn prevented formation of a complex between full-length ABAD and Aβ. This observation was consistent with the results in which we systematically administered mito-ABAD-DP to Tg mAPP mice. We propose that the presence of ABAD-DP or ABAD(92-120) in mitochondria prevented ABAD-Aβ complex formation, thereby preventing mitochondrial perturbation.

To further assess this concept, we evaluated mitochondrial function, including oxygen consumption, activity of the respiratory chain complexes, and generation of ROS. Consistent with our previous studies (Caspersen et al., 2005; Du et al., 2008, 2009), Tg mAPP mice at the age of 10–12 months displayed abnormal mitochondrial function as evidenced by the reduction in respiratory chain rate (Fig. 3C), and enzymatic activity of complex III–IV (supplemental Fig. S3A,B, available at www.jneurosci.org as supplemental material). However, mitochondria purified from double Tg mAPP/mito-ABAD animals demon-
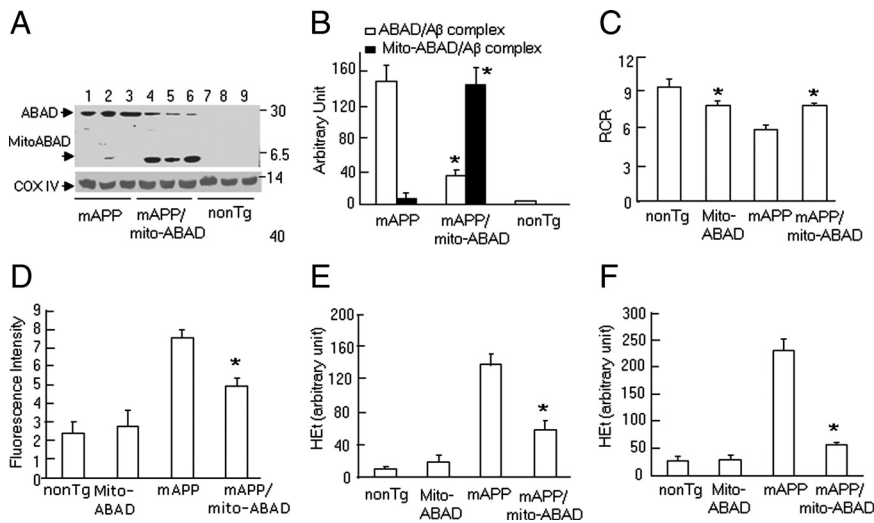
Figure 3. Expression of ABAD(92-120) reduces ABAD-Aβ complex formation, restores mitochondrial function, and attenuates generation of ROS. **A**, Immunoprecipitation of cortical mitochondria of the indicated Tg mice with 6E10 followed by immunoblotting with anti-ABAD showed two immunoreactive bands, $M_r \sim 27$ (ABAD/Aβ complex) and ~ 5 kDa [ABAD(92-120)/Aβ complex)]. Bottom shows immunoblotting of cortical mitochondrial fractions with α-COX IV. **B**, **C**, Quantification of intensity of immunoreactive bands corresponding to $M_r \sim 27$ and ~ 5 kDa (**B**) and oxygen consumption (**C**, respiratory control ratio) in cortical mitochondria from the indicated Tg mice. **D**, Fluorescence intensity of HEt (indicator of ROS) in brain homogenates. **E**, **F**, Quantification of area occupied by HEt staining in the cerebral cortex (**E**) and hippocampus (**F**) of the indicated Tg mice. *$p < 0.01$ vs Tg mAPP mice. $n = 3$–6 mice per group.

strated virtually complete preservation of oxygen consumption, as well as complex III and IV enzyme activity. Since overexpression of ABAD in Tg mAPP mice enhanced ROS generation (Yan et al., 1999; Lustbader et al., 2004), we examined whether blocking ABAD/Aβ interaction in Tg mAPP/mito-ABAD mice attenuated ROS production. Specifically, we studied mitochondria-derived ROS production using HEt, a fluorescent dye that is oxidized to ethidium selectively by superoxide (Murakami et al., 1998). Intravenous HEt injection was administered to mice followed by quantification of Het fluorescence intensity in the brain. Fluorescence intensity was significantly greater in brain homogenates of Tg mAPP mice than other groups of mice. However, there was an ~50% reduction of HEt fluorescent intensity in the brain of Tg mAPP/mito-ABAD mice compared with Tg mAPP mice (Fig. 3D). Quantification of the HEt-stained area in brain sections showed decreased superoxide production by 40% and 70%, respectively, in the cerebral cortex and the hippocampus of Tg mAPP/mito-ABAD mice, compared with those in the single Tg mAPP mice (Fig. 3 E, F). The fluorescent signals were distributed, at least in part, in mitochondria, as shown by colocalization of Hsp60 (a mitochondrial marker) with HEt staining (supplemental Fig. S3C–E, available at www.jneurosci.org as supplemental material), indicating mitochondrial production of superoxide. These data are consistent with the hypothesis that blockade of the interaction of intact ABAD with Aβ decreases generation of mitochondrial oxygen-free radicals.

Effect of transgene ABAD(92-120) on neuropathology and spatial learning/ memory in Tg mAPP/mito-ABAD mice

In view of the known exaggerated neuronal dysfunction and accelerated decline in spatial learning/memory induced by the ABAD-Aβ interaction (Lustbader et al., 2004; Chaney et al., 2005), we proposed that inhibition of this interaction would have a beneficial/protective effect on neuronal function. The density of cholinergic fibers and synapses is diminished in AD-like pathology and in accelerated AD-type mouse models (Geula, 1998;

Mucke et al., 2000; Arancio et al., 2004; Lustbader et al., 2004; Chaney et al., 2005; Yan and Stern, 2005; Fang et al., 2009). Thus, we measured AChE enzyme activity and semiquantitatively analyzed the density of AChE activity-positive neurites (which predominantly labels cholinergic neurites) in Tg mice using a standard histochemical method. AChE-positive neurites were shown as positively staining neurites in the subiculum. Consistent with our previous observations (Arancio et al., 2004; Yan and Stern, 2005; Fang et al., 2009), at 10–12 months of age, the area occupied by AChE-positive neurites in the subiculum was decreased in Tg mAPP mice ($p < 0.01$), compared with non-Tg littermates and Tg mito-ABAD mice (Fig. 4A). In contrast, double Tg mito-mAPP/mito-ABAD mice showed significantly less reduction in AChE-positive neurites (Fig. 4A). Representative images of AChE histochemically stained subiculum sections from each genotype are shown in supplemental Fig. S4, available at www.jneurosci.org as supplemental material. Consistent with histochemical studies, AChE activity was also significantly reduced in the subiculum region of Tg mAPP mice (Fig. 4B). Notably, non-Tg and Tg mito-ABAD mice do not display such abnormalities. Further, introduction of ABAD(92-120) attenuated this Aβ-mediated regional neuropathologic change, suggesting the critical role of mitochondrial Aβ interaction with ABAD.

To determine whether neuropathologic changes would be reflected in neuronal dysfunction, we performed behavioral analysis using the radial arm water maze to assess spatial learning/ memory in these Tg mice. At 10–12 months of age, non-Tg and Tg mito-ABAD mice displayed normal spatial learning as shown by an average of ~2–2.5 errors, whereas Tg mAPP mice averaged ~5–6 errors by trials 3–5, indicating impaired spatial memory for platform location between trials. However, double Tg mAPP/ mito-ABAD mice exhibited ~3 errors by trial 3–5 (Fig. 4C). Notably, Tg mito-ABAD and non-Tg littermates displayed identical performance in this behavioral task, suggesting that overexpression of ABAD(92-120) does not affect spatial memory. These data indicate that blockade of ABAD-Aβ interaction improves neuronal function, and learning/memory in mAPP mice.

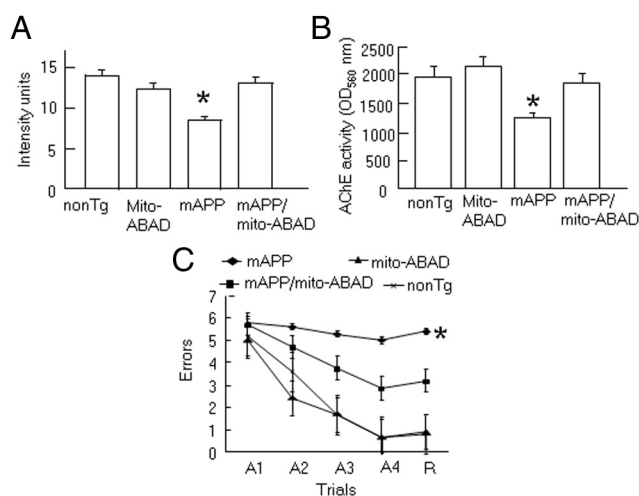### Antagonizing ABAD peptide reduces accumulation of mitochondrial Aβ and increases PreP activity in Tg mAPP mice

Since systemic administration of mito-ABAD-DP and overexpression of the ABAD(92-120) transgene in Tg mAPP mice significantly reduced ABAD-Aβ complex formation, we sought to determine the effect of this ABAD-derived peptide on mitochondrial Aβ accumulation. We encountered an unexpected finding that mitochondrial Aβ levels (including Aβ40 and -42) were significantly reduced in Tg mAPP mice treated with mito-ABAD-DP by 2- to 4-fold in the cortical mitochondrial fractions, but not in Tg mAPP mice treated with reversed control peptide, compared with single Tg mAPP mice (Fig. 5A, B). Similarly, Tg mAPP mice overexpressing ABAD(92-120) had significantly decreased levels of Aβ40 and Aβ42 by ~3- to 4-fold in the cortical mitochondrial fractions (Fig. 5C,D). These results indicate that

blockade of the ABAD-Aβ interaction in Tg mAPP mice diminished Aβ accumulation within mitochondria and led us to next determine the fate of mitochondrial Aβ in Tg mAPP mice overexpressing ABAD(92-120).

The presequence peptidase, PreP, is a recently identified novel mitochondrial peptidase responsible for degrading presequences and other short unstructured peptides (<70 aa) in mitochondria. The human PreP homolog (hPreP) is localized in the mitochondrial matrix and is a protease capable of degrading Aβ (Falkevall et al., 2006). We speculated that PreP might play a role in degrading mitochondrial Aβ in the *in vivo* environment, and may therefore be responsible for the reduction of mitochondrial Aβ levels seen in Tg mAPP mice expressing ABAD(92-120). Therefore, we performed a series of experiments to determine whether PreP plays a role in lowering mitochondrial Aβ in Tg mAPP/mito-ABAD mice. First, we examined PreP activity in Tg mAPP mice using a degradation assay. Brain mitochondria containing PreP isolated from Tg mice were incubated with a biotin-labeled Aβ42 peptide followed by pull-down of the biotin-labeled Aβ42 with avidin-conjugated agarose. Samples were then subjected to Western blot analysis to determine the capacity of mitochondrial PreP to degrade exogenous biotin-labeled Aβ42. PreP from non-Tg brain mitochondria revealed complete degradation of Aβ as demonstrated by undetectable or very weak Aβ-immunoreactive bands (Fig. 5*E*, lanes 4–7). In contrast, PreP from Tg mAPP mitochondria showed strong immunoreactive Aβ bands (Fig. 5*E*, lanes 8–11), suggesting that PreP degrading activity was significantly reduced in Tg mAPP mitochondria. Notably, PreP from Tg mAPP/mito-ABAD mitochondria was able to degrade Aβ by 80% compared with mAPP mitochondria (Fig. 5*E*, lanes 12–15, *F*), suggesting increased PreP activity in Tg mAPP/mito-ABAD mice. Quantification of the combined density of all immunoreactive bands is shown in Figure 5*F*. To determine the extent of PreP-dependent degradation of Aβ, we performed immunoinactivation assays with a specific antibody to PreP. In the absence of PreP antibody, we found that recombinant PreP protein (Fig. 5*E*, lane 2) or mitochondrial matrix PreP protein (Fig. 5*E*, lanes 4–7, *F*) almost completely degraded Aβ compared with samples without mitochondrial PreP protein (Fig. 5*E*, lane 1). Neutralization of the recombinant PreP protein or the mitochondrial matrix PreP protein with PreP antibody revealed an almost complete inhibition of the biotin-labeled Aβ42 degradation (Fig. 5*E*, lanes 3, 16–19, *F*). This result is demonstrated by Aβ-immunoreactive bands, indicating the specific effect of PreP on Aβ degradation.

Figure 4. Neuropathology and behavior in mAPP/mito-ABAD mice. *A*, AChE-positive neurites were visualized histochemically in the subiculum (Sb) of the indicated Tg mice. *B*, AChE activity in the subiculum of the indicated Tg mice. *p < 0.01 vs other groups of mice. *C*, Behavioral studies in Tg mice. Spatial learning and memory was tested in the radial arm water maze in the indicated Tg mice. A1–A4 denote the acquisition trials, and R denotes the retention trial. *p < 0.01 Tg mAPP mice vs other groups of mice. n = 4–8 mice per group.
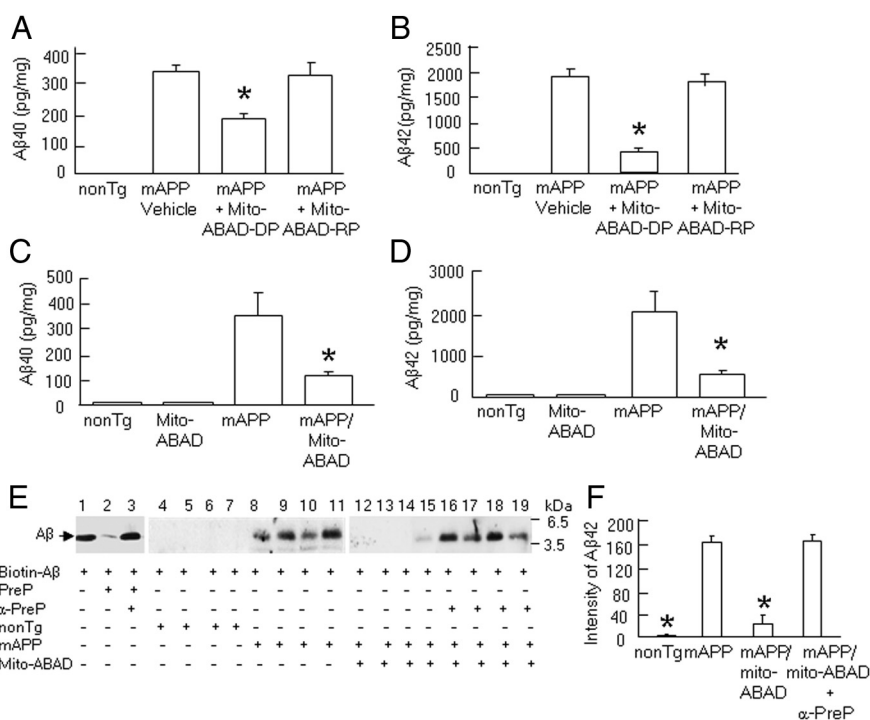
Figure 5. Effect of ABAD antagonizing peptide on accumulation of mitochondrial Aβ in Tg mAPP mice. *A*, *B*, ELISA for measurement of mitochondrial Aβ40 (*A*) and -42 (*B*) levels in Tg mAPP mice treated with Mito-ABAD-DP or -RP at age of 10–11 months. *p < 0.01 vs vehicle- or Mito-ABAD-RP-treated Tg mAPP mice. *C*, *D*, ELISA for Aβ40 (*C*) and Aβ42 (*D*) in the cortical mitochondria from the indicated Tg mice at 10–11 months old. *p < 0.01 vs Tg mAPP mice. *E*, PreP activity for degradation of biotin-Aβ. *F*, Quantification of density of all Aβ-immunoreactive bands incubated with mitochondrial fractions from non-Tg littermates (lanes 4–7), Tg mAPP mice (lanes 8–11), double Tg mAPP/mito-ABAD (lanes 12–15), and Tg mAPP/mito-ABAD plus anti-PreP antibody mice (lanes 16–19) using NIH ImageJ software. *p < 0.01 vs other groups of mice. n = 5–10 mice per group.

Discussion

The present study provides support for a pathologic role of the ABAD-Aβ interaction in promoting mitochondrial and neuronal dysfunction in an Aβ-rich environment, as shown in a mouse model of AD. We have demonstrated substantial evidence of the protective effect of blocking the ABAD-Aβ interaction using a combination of genetic and biochemical approaches applied to this mouse model.

Initially, using the yeast two-hybrid system, and, subsequently, by ligand binding assays with purified polypeptides and crystal structure analysis, our group identified an ABAD polypeptide capable of binding Aβ (Yan et al., 1997; Lustbader et al., 2004). Next, we identified an ABAD-Aβ complex *in vivo* in cortical mi-

tochondria from AD brain and transgenic AD mice (Lustbader et al., 2004). Importantly, the ABAD-Aβ interaction exacerbates mitochondrial and neuronal dysfunction in AD mice and in Aβ-induced neuronal injury (Yan et al., 1999; Lustbader et al., 2004; Takuma et al., 2005; Yan and Stern, 2005), indicating that the interaction of ABAD with Aβ is critical for facilitating Aβ-induced mitochondrial and neuronal stress. These studies raised the question as to whether the blockade of the ABAD-Aβ interaction might attenuate these deleterious effects observed in APP/Aβ mice or in Aβ-perturbed neurons.

To block ABAD-Aβ interaction, we used an ABAD decoy peptide to compete with and neutralize the binding of Aβ to endogenous full-length ABAD. The choice of peptide was guided by structural studies demonstrating that residues (94–114) of ABAD comprise the site of Aβ binding, and a peptide encompassing this region (residues 92-120) of human ABAD (ABAD-DP) inhibited binding of ABAD to Aβ based on surface plasmon resonance (Lustbader et al., 2004). Further *in vitro* experiments revealed that the addition of cell-permeable ABAD-DP, the latter with the cell-membrane transduction domain of HIV Tat protein, to cultured cortical neurons largely prevented Aβ-induced cytochrome *c* release, ROS production, and apoptosis (Lustbader et al., 2004).

In the present study, we demonstrate the protective effects of inhibition of ABAD-Aβ binding on mitochondrial properties and cognitive function in an *in vivo* setting. First, using a recombinant molecular technique, we constructed a biologically active ABAD(93-116) peptide fused to the HIV Tat transduction protein domain and a mitochondrial targeting sequence. The protein transduction domain embedded in the HIV Tat protein (47–57) has been successfully used to study intracellular mechanisms based on high efficiency (~90%) delivery of peptides/polypeptides both *in vitro* and *in vivo* (Lissy et al., 2000; Aarts et al., 2002; Cao et al., 2002; Wadia and Dowdy, 2002). It has been shown that Tat-linked proteins can penetrate the blood–brain barrier; thus Tat-mediated delivery of proteins/peptides holds potential for future therapeutic applications. The presence of the membrane transduction and mitochondrial targeting domains results in effective penetration and concentration of polypeptides into mitochondria in an intact tissue. As we observed, Tat-ABAD peptide was efficiently transduced to neurons and localized to mitochondria *in vitro* and *in vivo*.

Indeed, we have successfully used this decoy peptide before to demonstrate *in vivo* effects. Specifically, from a proteomic study of proteins with elevated expression in Tg mAPP/ABAD mice, we identified two proteins, peroxiredoxin II and endophilin I, present at higher levels in the cerebral cortex of Tg mAPP, Tg mAPP/ABAD mice and human AD patients (Yao et al., 2007; Ren et al., 2008). These two proteins typify the complex changes in protein expression in AD brain, as the expression of peroxiredoxin II and endophilin I has the potential to either promote or inhibit neuronal survival, respectively (Yao et al., 2007; Ren et al., 2008). Using the expression of these two proteins as a biological marker, we showed that the Tat-Mito-ABAD-DP decoy peptide, when injected intraperitoneally into Tg mAPP mice (using the same protocol as in the current study) had the ability to diminish expression of these two proteins to normal levels while the reverse peptide was inactive in this regard (Yao et al., 2007; Ren et al., 2008).

In this study, we have gone further and directly observed that introduction of ABAD decoy peptide *in vivo* dissociates ABAD from Aβ with resultant restoration of ABAD function and PreP activity. In parallel, treatment with the ABAD decoy peptide decreased formation of the ABAD-Aβ complex, restored mitochondrial respiratory function and enzyme activity, attenuated mitochondrial ROS production/accumulation, increased activity of Aβ degrading enzyme, and, presumably, thereby improved learning and memory. Similar results were observed in Tg mAPP mice overexpressing neuronal ABAD decoy peptide. Together, these observations confirm the protective effects of ABAD decoy peptide.

Intriguingly, mitochondrial Aβ levels were significantly lower in Tg mAPP mice treated with the ABAD decoy peptide or in mice expressing this peptide versus vehicle-treated mAPP mice. Furthermore, PreP proteolytic activity was decreased in Aβ-rich mitochondria, but was significantly enhanced in the presence of the ABAD decoy peptide. It has been demonstrated that human PreP is the sole Aβ-degrading protease responsible for degradation and clearance of Aβ in mitochondria recognized to date. Impaired PreP activity would therefore promote accumulation of Aβ, ultimately causing aberrant mitochondrial and neuronal function (Falkevall et al., 2006). *In situ* immunoinactivation studies using anti-PreP antibody eliminated degradation of Aβ, proving that PreP is necessary for the clearance of Aβ in mitochondria. Thus, decreased PreP activity may be an important mechanism underlying Aβ accumulation in mitochondria in mAPP mice.

Given that proteolytic activity of PreP under oxidizing conditions was associated with Aβ accumulation (Falkevall et al., 2006), we predicted that diminished PreP activity, observed in the presence of ABAD-Aβ complex (i.e., in Tg mAPP mice), would occur in tandem with higher levels of mitochondrial ROS. Consistent with this concept, in the presence of ABAD-DP (which dissociated the complex between full-length ABAD and Aβ), levels of ROS were reduced and PreP demonstrated the ability to degrade Aβ. These data are also consistent with the changes in mitochondrial Aβ levels in Tg mice, which were elevated in Tg mAPP mice and reduced by administration of mito-ABAD-DP.

Together, these findings provide substantial evidence of the protective effect of inhibition of ABAD-Aβ interaction on mitochondrial, neuronal, and cognitive function in an AD mouse model. Most importantly, we demonstrated that blockade of ABAD-Aβ interaction reduces mitochondrial Aβ accumulation, leading to improvement in mitochondrial function, attenuation of mitochondrial ROS production, and increased PreP activity. Elevated levels of oxidative stress in mitochondria due to a direct effect of Aβ or ABAD-Aβ interaction may be responsible for decreased PreP activity, which in turn leads to further accumulation of Aβ, and exacerbates mitochondrial and neuronal dysfunction, all of which contribute to the picture of AD pathogenesis. These results provide the first mechanistic insight into Aβ perturbation of mitochondrial function in AD. One or more agents that block ABAD-Aβ interaction may therefore be potential therapeutic approaches for preventing and/or halting AD progression.

References

Aarts M, Liu Y, Liu L, Besshoh S, Arundine M, Gurd JW, Wang YT, Salter MW, Tymianski M (2002) Treatment of ischemic brain damage by perturbing NMDA receptor-PSD-95 protein interactions. Science 298:846–850.

Arancio O, Zhang HP, Chen X, Lin C, Trinchese F, Puzzo D, Liu S, Hegde A, Yan SF, Stern A, Luddy JS, Lue LF, Walker DG, Roher A, Buttini M, Mucke L, Li W, Schmidt AM, Kindy M, Hyslop PA, et al. (2004) RAGE potentiates Abeta-induced perturbation of neuronal function in transgenic mice. EMBO J 23:4096–4105.

Beal MF (2004) Mitochondrial dysfunction and oxidative damage in Alz-

heimer's and Parkinson's diseases and coenzyme Q10 as a potential treatment. J Bioenerg Biomembr 36:381–386.

Birch-Machin MA, Turnbull DM (2001) Assaying mitochondrial respiratory complex activity in mitochondria isolated from human cells and tissues. Methods Cell Biol 65:97–117.

Blass JP (2000) The mitochondrial spiral. An adequate cause of dementia in the Alzheimer's syndrome. Ann N Y Acad Sci 924:170–183.

Bosetti F, Brizzi F, Barogi S, Mancuso M, Siciliano G, Tendi EA, Murri L, Rapoport SI, Solaini G (2002) Cytochrome c oxidase and mitochondrial F1F0-ATPase (ATP synthase) activities in platelets and brain from patients with Alzheimer's disease. Neurobiol Aging 23:371–376.

Cao G, Pei W, Ge H, Liang Q, Luo Y, Sharp FR, Lu A, Ran R, Graham SH, Chen J (2002) In vivo delivery of a Bcl-xL fusion protein containing the TAT protein transduction domain protects against ischemic brain injury and neuronal apoptosis. J Neurosci 22:5423–5431.

Caspersen C, Wang N, Yao J, Sosunov A, Chen X, Lustbader JW, Xu HW, Stern D, McKhann G, Yan SD (2005) Mitochondrial Abeta: a potential focal point for neuronal metabolic dysfunction in Alzheimer's disease. FASEB J 19:2040–2041.

Chaney MO, Stine WB, Kokjohn TA, Kuo YM, Esh C, Rahman A, Luehrs DC, Schmidt AM, Stern D, Yan SD, Roher AE (2005) RAGE and amyloid beta interactions: atomic force microscopy and molecular modeling. Biochim Biophys Acta 1741:199–205.

Chen JX, Yan SD (2007) Amyloid-beta-induced mitochondrial dysfunction. J Alzheimers Dis 12:177–184.

Davis RE, Miller S, Herrnstadt C, Ghosh SS, Fahy E, Shinobu LA, Galasko D, Thal LJ, Beal MF, Howell N, Parker WD JR (1997) Mutations in mitochondrial cytochrome c oxidase genes segregate with late-onset Alzheimer disease. Proc Natl Acad Sci U S A 94:4526–4531.

Devi L, Prabhu BM, Galati DF, Avadhani NG, Anandatheerthavarada HK (2006) Accumulation of amyloid precursor protein in the mitochondrial import channels of human Alzheimer's disease brain is associated with mitochondrial dysfunction. J Neurosci 26:9057–9068.

Du H, Guo L, Fang F, Chen D, Sosunov AA, McKhann GM, Yan Y, Wang C, Zhang H, Molkentin JD, Gunn-Moore FJ, Vonsattel JP, Arancio O, Chen JX, Yan SD (2008) Cyclophilin D deficiency attenuates mitochondrial and neuronal perturbation and ameliorates learning and memory in Alzheimer's disease. Nat Med 14:1097–1105.

Du H, Guo L, Zhang W, Rydzewska M, and Yan S (2009) Cyclophilin D deficiency improves mitochondrial function and learning/memory in aging Alzheimer disease mouse model. Neurobiology Aging. Advance online publication. doi:10.1016/j.neurobiolaging.2009.03.003.

Falkevall A, Alikhani N, Bhushan S, Pavlov PF, Busch K, Johnson KA, Eneqvist T, Tjernberg L, Ankarcrona M, Glaser E (2006) Degradation of the amyloid beta-protein by the novel mitochondrial peptidasome, PreP. J Biol Chem 281:29096–29104.

Fang F, Flegler AJ, Du P, Lin S, Clevenger CV (2009) Expression of cyclophilin B is associated with malignant progression and regulation of genes implicated in the pathogenesis of breast cancer. Am J Pathol 174:297–308.

Floyd RA, Hensley K (2002) Oxidative stress in brain aging. Implications for therapeutics of neurodegenerative diseases. Neurobiol Aging 23:795–807.

Geula C (1998) Abnormalities of neural circuitry in Alzheimer's disease: hippocampus and cortical cholinergic innervation. Neurology 51 [Suppl 1]:S18–S29.

Hansson Petersen CA, Alikhani N, Behbahani H, Wiehager B, Pavlov PF, Alafuzoff I, Leinonen V, Ito A, Winblad B, Glaser E, Ankarcrona M (2008) The amyloid beta-peptide is imported into mitochondria via the TOM import machinery and localized to mitochondrial cristae. Proc Natl Acad Sci U S A 105:13145–13150.

He XY, Wen GY, Merz G, Lin D, Yang YZ, Mehta P, Schulz H, Yang SY (2002) Abundant type 10 17 beta-hydroxysteroid dehydrogenase in the hippocampus of mouse Alzheimer's disease model. Brain Res Mol Brain Res 99:46–53.

Hirai K, Aliev G, Nunomura A, Fujioka H, Russell RL, Atwood CS, Johnson AB, Kress Y, Vinters HV, Tabaton M, Shimohama S, Cash AD, Siedlak SL, Harris PL, Jones PK, Petersen RB, Perry G, Smith MA (2001) Mitochondrial abnormalities in Alzheimer's disease. J Neurosci 21:3017–3023.

Humphries KM, Szweda LI (1998) Selective inactivation of alpha-ketoglutarate dehydrogenase and pyruvate dehydrogenase: reaction of lipoic acid with 4-hydroxy-2-nonenal. Biochemistry 37:15835–15841.

Lin MT, Beal MF (2006) Alzheimer's APP mangles mitochondria. Nat Med 12:1241–1243.

Lissy NA, Davis PK, Irwin M, Kaelin WG, Dowdy SF (2000) A common E2F-1 and p73 pathway mediates cell death induced by TCR activation. Nature 407:642–645.

Lustbader JW, Cirilli M, Lin C, Xu HW, Takuma K, Wang N, Caspersen C, Chen X, Pollak S, Chaney M, Trinchese F, Liu S, Gunn-Moore F, Lue LF, Walker DG, Kuppusamy P, Zewier ZL, Arancio O, Stern D, Yan SS, et al. (2004) ABAD directly links Abeta to mitochondrial toxicity in Alzheimer's disease. Science 304:448–452.

Manczak M, Anekonda TS, Henson E, Park BS, Quinn J, Reddy PH (2006) Mitochondria are a direct site of A beta accumulation in Alzheimer's disease neurons: implications for free radical generation and oxidative damage in disease progression. Hum Mol Genet 15:1437–1449.

Maurer I, Zierz S, Möller HJ (2000) A selective defect of cytochrome c oxidase is present in brain of Alzheimer disease patients. Neurobiol Aging 21:455–462.

Mucke L, Masliah E, Yu GQ, Mallory M, Rockenstein EM, Tatsuno G, Hu K, Kholodenko D, Johnson-Wood K, McConlogue L (2000) High-level neuronal expression of abeta 1-42 in wild-type human amyloid protein precursor transgenic mice: synaptotoxicity without plaque formation. J Neurosci 20:4050–4058.

Murakami K, Kondo T, Kawase M, Li Y, Sato S, Chen SF, Chan PH (1998) Mitochondrial susceptibility to oxidative stress exacerbates cerebral infarction that follows permanent focal cerebral ischemia in mutant mice with manganese superoxide dismutase deficiency. J Neurosci 18:205–213.

Ren Y, Xu HW, Davey F, Taylor M, Aiton J, Coote P, Fang F, Yao J, Chen D, Chen JX, Yan SD, Gunn-Moore FJ (2008) Endophilin I expression is increased in the brains of Alzheimer disease patients. J Biol Chem 283:5685–5691.

Sheehan JP, Swerdlow RH, Miller SW, Davis RE, Parks JK, Parker WD, Tuttle JB (1997) Calcium homeostasis and reactive oxygen species production in cells transformed by mitochondria from individuals with sporadic Alzheimer's disease. J Neurosci 17:4612–4622.

Shukkur EA, Shimohata A, Akagi T, Yu W, Yamaguchi M, Murayama M, Chui D, Takeuchi T, Amano K, Subramhanya KH, Hashikawa T, Sago H, Epstein CJ, Takashima A, Yamakawa K (2006) Mitochondrial dysfunction and tau hyperphosphorylation in Ts1Cje, a mouse model for Down syndrome. Hum Mol Genet 15:2752–2762.

Takuma K, Yao J, Huang J, Xu H, Chen X, Luddy J, Trillat AC, Stern DM, Arancio O, Yan SS (2005) ABAD enhances Abeta-induced cell stress via mitochondrial dysfunction. FASEB J 19:597–598.

Wadia JS, Dowdy SF (2002) Protein transduction technology. Curr Opin Biotechnol 13:52–56.

Yan SD, Stern DM (2005) Mitochondrial dysfunction and Alzheimer's disease: role of amyloid-beta peptide alcohol dehydrogenase (ABAD). Int J Exp Pathol 86:161–171.

Yan SD, Fu J, Soto C, Chen X, Zhu H, Al-Mohanna F, Collison K, Zhu A, Stern E, Saido T, Tohyama M, Ogawa S, Roher A, Stern D (1997) An intracellular protein that binds amyloid-beta peptide and mediates neurotoxicity in Alzheimer's disease. Nature 389:689–695.

Yan SD, Shi Y, Zhu A, Fu J, Zhu H, Zhu Y, Gibson L, Stern E, Collison K, Al-Mohanna F, Ogawa S, Roher A, Clarke SG, Stern DM (1999) Role of ERAB/L-3-hydroxyacyl-coenzyme A dehydrogenase type II activity in Abeta-induced cytotoxicity. J Biol Chem 274:2145–2156.

Yan SD, Xiong WC, Stern DM (2006) Mitochondrial amyloid-beta peptide: pathogenesis or late-phase development? J Alzheimers Dis 9:127–137.

Yao J, Taylor M, Davey F, Ren Y, Aiton J, Coote P, Fang F, Chen JX, Yan SD, Gunn-Moore FJ (2007) Interaction of amyloid binding alcohol dehydrogenase/Abeta mediates up-regulation of peroxiredoxin II in the brains of Alzheimer's disease patients and a transgenic Alzheimer's disease mouse model. Mol Cell Neurosci 35:377–382.

Yao J, Irwin RW, Zhao L, Nilsen J, Hamilton RT, Brinton RD (2009) Mitochondrial bioenergetic deficit precedes Alzheimer's pathology in female mouse model of Alzheimer's disease. Proc Natl Acad Sci U S A 106:14670–14675.

Yao J, Hamilton RT, Cadenas E, Brinton RD (2010) Decline in mitochondrial bioenergetics and shift to ketogenic profile in brain during reproductive senescence. Biochim Biophys Acta 1800:1121–1126.